

Synthesis of Thieno-Bridged Porphyrins: Changing the Antiaromatic Contribution by the Direction of the Thiophene Ring

Yusuke Mitsushige,[†] Shigeru Yamaguchi,[†] Byung Sun Lee,[‡] Young Mo Sung,[‡] Susanne Kuhri,[§] Christoph A. Schierl,[§] Dirk M. Guldi,^{*,§} Dongho Kim,^{*,‡} and Yutaka Matsuo^{*,†}

[†]Department of Chemistry, School of Science, The University of Tokyo, Hongo, Bunkyo-Ku, Tokyo 113-0033, Japan

[‡]Department of Chemistry, Yonsei University, Seoul 120-749, Korea

[§]Department of Chemistry and Pharmacy and Interdisciplinary Center for Molecular Materials, Friedrich-Alexander-Universität Erlangen-Nürnberg, Egerlandstraße 3, 91058 Erlangen, Germany

S Supporting Information

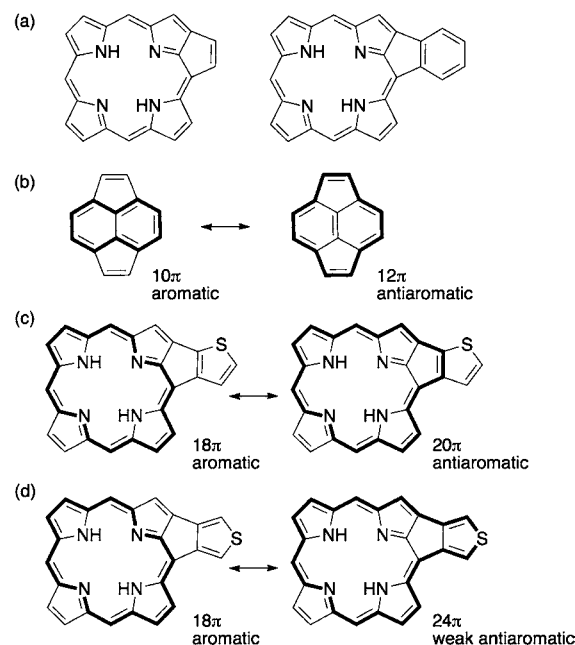
ABSTRACT: Two types of thieno-bridged porphyrins were synthesized by incorporating a thiophene group across their meso and β positions with different directions of the thiophene ring to investigate the aromaticity of these porphyrins with extended π -systems. The 2,3-thieno-bridged porphyrin showed a larger antiaromatic contribution than did the 3,4-thieno-bridged porphyrin. In the former, the antiaromatic contribution is based on a 20π -electron conjugated circuit. The two thieno-bridged porphyrins were characterized by calculations of nucleus-independent chemical shift and anisotropy of the induced current density as well as by X-ray crystallography, NMR spectroscopy, UV-vis-NIR absorption spectroscopy, electrochemical studies, time-resolved excited-state analysis, and two-photon absorption cross section measurements. Chemical derivatization of the 2,3-thieno-bridged porphyrin was also demonstrated.

Porphyrin is a representative π -functional skeleton that has been actively investigated in various fields of chemistry. To improve upon the properties of this macrocycle, extension of the π conjugation is a commonly used method.¹ In some cases, only a small extension of the porphyrin π system leads to largely altered properties. For instance, the properties of the macrocycle are substantially perturbed when an olefin² or phenyl³ moiety is incorporated across the meso and β positions (Chart 1a). These peripherally functionalized porphyrins bearing a fused five-membered ring have been known to have unusual properties such as largely altered light absorption extending to the far-red region.³ Although disrupted aromatic character has been suggested in such compounds,^{3d} the origin of the unusual properties has yet to be fully explained.

Pyracylene, which is one compound that shows such unusual properties, provides a clue for solving this problem. In the resonance structures of pyracylene, both aromatic 10π -electron (10π) and antiaromatic 12π circuits can be drawn (Chart 1b). The anomalous aromaticity of pyracylene has been a matter of debate since it was first synthesized in 1967.^{4,5}

In this paper, we will rationalize such unusual properties and aromaticity with the aid of rationally designed porphyrin derivatives. To this end, we synthesized two types of thieno-

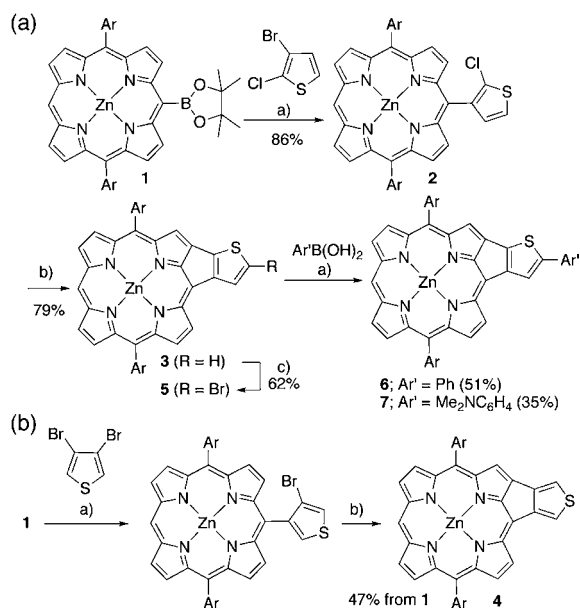
Chart 1. π -Extended Porphyrins and Pyracylene with Resonance Structures: (a) Porphyrins with a Double Bond Extending the π Network; (b) Pyracylene; (c) 2,3-Thieno-Bridged Porphyrin 3; (d) 3,4-Thieno-Bridged Porphyrin 4



bridged porphyrins (Chart 1c,d). The notable characteristic of the thieno-bridged porphyrins is that the π network can be manipulated by changing direction of the thiophene ring while maintaining the same size of the π faces. In this way, we can examine the effects of the additional π networks on the overall electronic structures of porphyrins. In the compound shown in Chart 1c, an antiaromatic 20π circuit would contribute to the overall electronic structure, while in the compound shown in Chart 1d, antiaromaticity would be weakened or disrupted by the sulfur atom on the 24π conjugated pathway, leading to normal or slightly perturbed aromatic character of the porphyrin macrocycle. To test this working hypothesis, we

Received: August 21, 2012

Published: September 18, 2012

Scheme 1. Synthesis and Further Functionalization of Thieno-Bridged Porphyrins^a

^aReagents and conditions: (a) Pd₂dba₃, PPh₃, Cs₂CO₃, toluene/DMF, 100 °C; (b) Pd(OAc)₂, PCy₃·HBF₄, K₂CO₃, DMF, 155 °C; (c) *N*-bromosuccinimide, CHCl₃, pyridine, 0 °C. Ar = 3,5-di-*tert*-butylphenyl.

synthesized these π -extended porphyrins and evaluated their aromaticities.

Our synthetic strategy for the thieno-bridged porphyrins is shown in Scheme 1. Suzuki–Miyaura cross-coupling of meso-borylporphyrin **1** with 2-chloro-3-bromothiophene and 3,4-dibromothiophene followed by intramolecular Heck reactions⁶ afforded 2,3- and 3,4-thieno-bridged porphyrins **3** and **4**, respectively, in yields of 68 and 47% over two steps. Crystal structures of their analogues **3'** and **4'** are shown in Figure 1a–d.⁷

According to calculations, pyracylene has a paratropic ring current on its five-membered rings as a result of superposition of 10π and 12π conjugated circuits.^{5d} We expected that superposition of 18π and 20π conjugated circuits in **3** would lead to a similar phenomenon, meaning that a paratropic ring current would be generated on the five-membered ring between the porphyrin and thiophene moieties (Figure S18 in the Supporting Information). To examine this hypothesis, we calculated the anisotropy of the induced current density (AICD), which represents the three-dimensional delocalized electron density with a scalar field and illustrates the paramagnetic term of the induced current density; aromatic molecules show clockwise current density and antiaromatic species show counterclockwise current density.^{8,9} AICD plots for **3** and **4** are shown in Figure 2. On the porphyrin macrocycles of both **3** and **4**, clockwise current density was observed, indicating that **3** and **4** are, on the whole, aromatic. Remarkably, in line with our expectations, counterclockwise current density was observed on the five-membered ring between the porphyrin and thiophene moieties of **3**, whereas in the AICD plot of **4**, clear current density was observed on only the porphyrin skeleton.

For **3** and **4**, we also calculated values of the nucleus-independent chemical shift (NICS), which has been success-

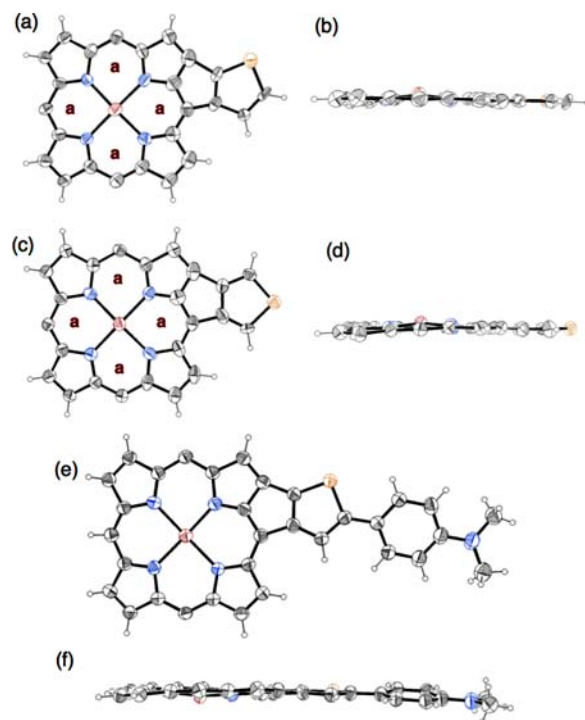


Figure 1. ORTEP drawings of **3'** [(a) top view; (b) side view], **4'** [(c) top view; (d) side view], and **7** [(e) top view; (f) side view]. The meso-aryl substituents have been omitted for clarity. The thermal ellipsoids are scaled to the 50% probability level.

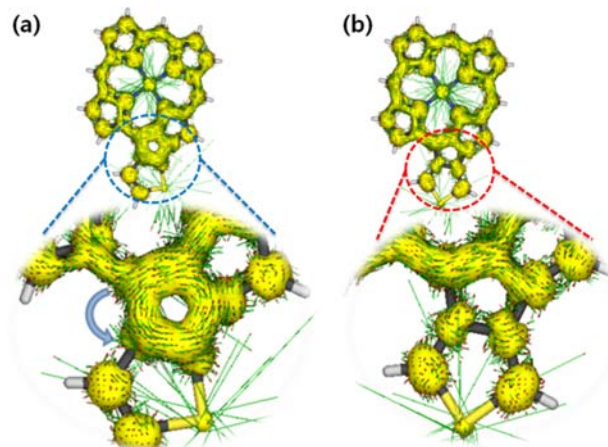


Figure 2. AICD plots for (a) **3** and (b) **4** at an isosurface value of 0.05.

fully used as a measure of aromaticity.¹⁰ At the five-membered ring between the porphyrin and thiophene moieties, the NICS(0) values for both **3** and **4** are positive (+30.5 and +13.1 ppm, respectively). The large positive NICS(0) value for **3** indicates a large contribution from the antiaromatic 20π circuit. A smaller contribution from the antiaromatic 24π circuit of **4** is also possible, judging from the positive value at the five-membered ring between the porphyrin and thiophene moieties of **4**. The NICS(0) values at the porphyrin macrocycle of **3** are more positive (−10.1 to −13.6 ppm; points “a” in Figure 1a) than those of **4** (−14.6 to −16.1 ppm; points “a” in Figure 1c), suggesting that the antiaromatic network makes a larger contribution to the overall electronic structure in **3** than in **4**.

One of the most useful experimental methods for assessing aromaticity is ¹H NMR spectroscopy. A paratropic ring current

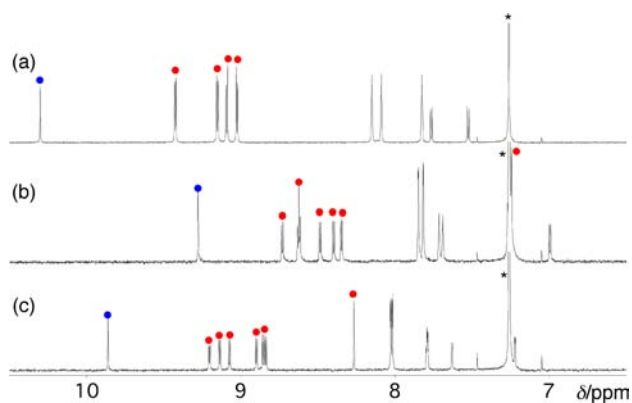


Figure 3. ^1H NMR spectra of (a) **2**, (b) **3**, and (c) **4** in CDCl_3 . Red and blue dots indicate signals of the porphyrin β and meso protons, respectively.

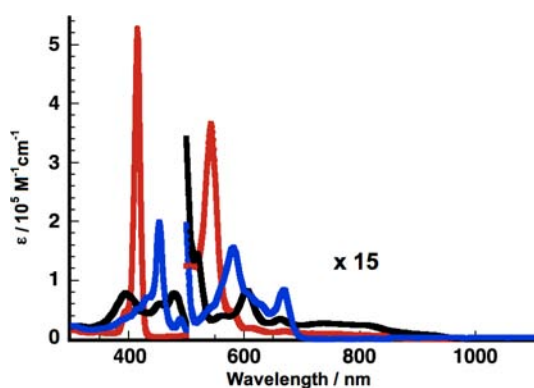


Figure 4. UV-vis-NIR absorption spectra of **2** (red), **3** (black), and **4** (blue) in CH_2Cl_2 .

shifts the signals of the peripheral protons on arenes upfield, and a diamagnetic ring current shifts them downfield. The ^1H NMR spectra of **2**, **3**, and **4** in CDCl_3 are shown in Figure 3. The signals of the meso and β protons are shifted further upfield in the order $2 < 4 < 3$, corresponding to the increasing contributions of antiaromaticity in resonance.

Recent studies of antiaromatic and aromatic porphyrinoids have revealed that UV-vis-NIR absorption spectroscopy is helpful in distinguishing between them.¹¹ UV-vis-NIR absorption spectra of **2**, **3**, and **4** are shown in Figure 4. Compound **2** showed Soret and Q bands, which are typical of aromatic porphyrins. Soret and Q bands were also observed in the spectrum of **4**, but both bands were weaker and broader in comparison with those of **2**. Compounds **2** and **4** exhibited fluorescence maxima at 588 and 674 nm and fluorescence quantum yields of 0.014 and 0.009, respectively. In contrast, the optical properties of **3** were markedly different from those of **2** and **4**. The Soret and Q bands of **3** were notably attenuated. Moreover, weak NIR absorption appeared, with the absorption edge extending to 1000 nm. No fluorescence was observed. Interestingly, changing the direction of the thiophene moiety induced major differences in the optical properties. It is also noteworthy that the optical properties of **3** closely resemble those of antiaromatic porphyrinoids, which exhibit no fluorescence and have broad Soret bands and featureless, smeared Q-like bands.¹¹

To gain insight into the absorption spectra, molecular orbital (MO) and time-dependent density functional theory (TD-

DFT) calculations on **3** and **4** were performed at the B3LYP/6-31G* level. The calculated transitions agreed fairly well with the experimental absorption spectra in terms of both position and relative intensity. Compared with **4**, which maintained the degeneracy of its frontier MOs as a typical porphyrinoid system does, thieno-bridged porphyrin **3** showed a relatively broken degeneracy between the lowest unoccupied MO (LUMO) and the LUMO+1 as well as between the highest occupied MO (HOMO) and the HOMO-1, which accounts for the red-shifted absorption of **3**.

The electrochemical properties of **2**, **3**, and **4** were examined by cyclic voltammetry. The first oxidation waves (E_{ox1}) of **2** and **4** were observed at 0.38 and 0.25 V vs ferrocene/ferrocenium (Fc/Fc^+), respectively. In comparison with the first oxidation potentials of **2** and **4**, that of **3** was found to be substantially more negative (0.02 V vs Fc/Fc^+).¹² The first reduction waves (E_{red1}) of **2**, **3**, and **4** were observed at -1.83, -1.57, and -1.68 V vs Fc/Fc^+ , respectively. ΔE ($E_{\text{ox1}} - E_{\text{red1}}$) decreased in the order 2 ($\Delta E = 2.21$ eV) $>$ 4 ($\Delta E = 1.93$ eV) $>$ 3 ($\Delta E = 1.59$ eV), consistent with the UV-vis absorption spectra.

Femtosecond transient absorption (fs-TA) and time-resolved fluorescence measurements were carried out in toluene at room temperature to explore the photophysics of the aromaticity-dependent excited states in the compounds. As expected from the results described above, the temporal decay profiles of thieno-bridged porphyrins **3** and **4** also indicated quite different properties. The singlet excited state lifetime of **4** was evaluated as 790 ps by monoexponential fits of the time-resolved fluorescence and fs-TA decay profiles, but the fs-TA decay profile of **3** had to be fit using a double-exponential decay function, revealing two time constants with values of 850 fs and 7.5 ps. The femtosecond time constant of **3** corresponds to the internal conversion time from the Q-like state to the lowest S_1 state (700–1000 nm), while the picosecond time constant corresponds to the lifetime of the lowest S_1 state, as in the profiles of antiaromatic porphyrinoids.¹¹ In addition to these fast decay profiles, we observed additional long time constants from fs-TA measurements of both **3** and **4**. These other time constants are attributable to triplet excited state lifetimes. Thus, nanosecond-transient absorption (ns-TA) measurements were also carried out. Here, a triplet excited state lifetime of 1.9 μs for **3** was found from its ns-TA decay profile; this lifetime is slightly shorter than that of **4** (2.5 μs). The singlet and triplet excited state lifetimes of the two thieno-bridged porphyrins **3** and **4** are shorter than those of Zn(II) tetraphenylporphyrin (2 ns and 1 ms, respectively). The shorter S_1 lifetime for **3** than for **4** is consistent with the lack of fluorescence in **3**. This optical properties of **3** arise in part from the acceleration of nonradiative internal conversion from the S_1 state to the S_0 state due to the reduction in the energy gap caused by breaking of the frontier orbital degeneracy as a result of the strong antiaromaticity of **3**. The shorter lifetimes of the triplet excited states in both cases essentially arise from the heavy-atom effect of sulfur in the bridging thiophenes.

Antiaromaticity of porphyrinoids leads to significant changes in not only the linear optical properties but also the nonlinear ones.¹¹ Thus, the two-photon absorption (TPA) cross sections of **3** and **4** were measured by the wavelength-scanning open-aperture Z-scan method over wavelength ranges of 1100–1600 and 900–1350 nm, respectively, where the contribution of one-photon absorption is negligible. Despite the similar structures of these compounds, **3** exhibited a small TPA cross section of 200 GM (1 GM = 10^{-50} $\text{cm}^4 \text{s photon}^{-1}$) at the lowest-energy

TPA band maximum, which is only about one-third of the value of the TPA cross section of **4** at the same position (550 GM), suggesting that the electronic delocalization in **3** is quite unique and different from that of **4**. However, at 1300 nm, corresponding to the Q-like band, the TPA cross sections of **3** and **4** are roughly the same (400 and 550 GM, respectively). In other words, the TPA cross sections in the Q-like band region are mainly affected by Zn(II) porphyrin moieties.

Overall, we propose that the unusual properties of porphyrins that are peripherally functionalized with a fused five-membered ring come from the 20π conjugated antiaromatic circuit, which was characterized by the theoretical and experimental investigations described above. More importantly, through a comparison with 3,4-thieno compound **4**, the antiaromatic contribution of the 20π circuit in **3** was clearly elucidated.

Lastly, we examined the reactivity of thieno-bridged porphyrin **3**. As shown in Scheme 1a, bromination of **3** with *N*-bromosuccinimide occurred at the α position of the thiophene moiety, affording brominated thieno-bridged porphyrin **5** in 62% yield. Cross-coupling reactions of **5** would enable the introduction of various substituents, thereby giving a means of further understanding this unique aromaticity. In fact, phenyl and (dimethylamino)phenyl substituents could be introduced via Suzuki–Miyaura coupling to afford **6** (51%) and **7** (35%). The X-ray crystal structure of **7** is shown in Figure 1e,f. The anomalous aromaticity of **3** was retained in the products **6** and **7**, as confirmed by their ^1H NMR and UV–vis–NIR absorption spectra.

In conclusion, we have employed the concept of antiaromaticity to rationalize the unusual properties of peripherally π -extended porphyrins. To examine the antiaromatic contribution in π -extended porphyrins, we synthesized 2,3- and 3,4-thieno-bridged porphyrins, which have different directions of the thiophene ring and the same size of the π faces. The former compound showed a clear antiaromatic contribution due to its 20π conjugated circuit, whereas the latter exhibited a lesser contribution of antiaromaticity because of the disruption of the possible 24π antiaromatic circuit by the sulfur atom. These results provide a useful guideline for controlling the properties of porphyrins, an important class of π -functional molecules.

■ ASSOCIATED CONTENT

■ Supporting Information

General synthetic procedures, NMR and UV–vis–NIR spectra, cyclic voltammograms, time-resolved photophysics data, theoretical calculation data, and CIF files for **3'**, **4'**, and **7**. This material is available free of charge via the Internet at <http://pubs.acs.org>.

■ AUTHOR INFORMATION

Corresponding Author

guldi@chemie.uni-erlangen.de; dongho@yonsei.ac.kr; matsuo@chem.s.u-tokyo.ac.jp

Notes

The authors declare no competing financial interest.

■ ACKNOWLEDGMENTS

This work was supported by the Funding Program for Next-Generation World-Leading Researchers. We thank Prof. Hiroshi Shinokubo (Nagoya University) for conducting ESI-TOF-MS measurements. The work at Yonsei University was

supported by the Midcareer Researcher Program (2010-0029668) and the World Class University Program (R32-2010-000-10217) of the Ministry of Education, Science, and Technology (MEST) of Korea. The quantum calculations were performed using the supercomputing resources of the Korea Institute of Science and Technology Information (KISTI). This work was also supported in part by the Deutsche Forschungsgemeinschaft Cluster of Excellence “Engineering of Advanced Materials” and NDRL, which is supported by the Division of Chemical Sciences, Geosciences and Biosciences, Basic Energy Sciences, Office of Science, United States Department of Energy through grant number DE-FC02-04ER15533.

■ REFERENCES

- (1) (a) Lewtak, J. P.; Gryko, D. T. *Chem. Commun.* **2012**, *48*, 10069. (b) Aratani, N.; Kim, D.; Osuka, A. *Chem.—Asian J.* **2009**, *4*, 1172. (c) Senge, M. O.; Fazekas, M.; Notaras, E. G. A.; Blau, W. J.; Zawadzka, M.; Locos, O. B.; Mhuirheartaigh, E. M. N. *Adv. Mater.* **2007**, *19*, 2737. (d) Pawlicki, M.; Collins, H. A.; Denning, R. G.; Anderson, H. L. *Angew. Chem., Int. Ed.* **2009**, *48*, 3244.
- (2) (a) Sahoo, A. K.; Mori, S.; Shinokubo, H.; Osuka, A. *Angew. Chem., Int. Ed.* **2006**, *45*, 7972. (b) Nakano, A.; Aratani, N.; Furuta, H.; Osuka, A. *Chem. Commun.* **2001**, 1920.
- (3) (a) Fox, S.; Boyle, R. W. *Chem. Commun.* **2004**, 1322. (b) Shen, D.-M.; Liu, C.; Chen, Q.-Y. *Chem. Commun.* **2005**, 4982. (c) Hayashi, S.; Matsubara, Y.; Eu, S.; Hayashi, H.; Umeyama, T.; Matano, Y.; Imahori, H. *Chem. Lett.* **2008**, *37*, 846. (d) Lash, T. D.; Smith, B. E.; Melquist, M. J.; Godfrey, B. A. *J. Org. Chem.* **2011**, *76*, 5335.
- (4) (a) Trost, B. M.; Bright, G. M. *J. Am. Chem. Soc.* **1967**, *89*, 4244. (b) Trost, B. M.; Bright, G. M.; Frihart, C.; Britteli, D. R. *J. Am. Chem. Soc.* **1971**, *93*, 737.
- (5) (a) Freiermuth, B.; Gerber, S.; Riesen, A.; Wirz, J.; Zehnder, M. *J. Am. Chem. Soc.* **1990**, *112*, 738. (b) Diogo, H. P.; Kiyobayashi, T.; Minas da Piedade, M. E.; Burlak, N.; Rogers, D. W.; McMasters, D.; Persy, G.; Wirz, J.; Liebman, J. F. *J. Am. Chem. Soc.* **2002**, *124*, 2065. (c) Randić, M. *Chem. Rev.* **2003**, *103*, 3449. (d) Steiner, E.; Fowler, P. W. *J. Phys. Chem. A* **2001**, *105*, 9553.
- (6) Campeau, L.-C.; Parisien, M.; Jean, A.; Fagnou, K. *J. Am. Chem. Soc.* **2006**, *128*, 581.
- (7) Crystals suitable for X-ray diffraction analysis could not be obtained from the 5,15-diaryl-substituted thieno-bridged porphyrins **3** and **4**, but we were able to obtain the crystal structures of the 5,10,15-triaryl-substituted analogues **3'** and **4'**.
- (8) (a) Geuenich, D.; Hess, K.; Köhler, F.; Herges, R. *Chem. Rev.* **2005**, *105*, 3758. (b) Herges, R.; Geuenich, D. *J. Phys. Chem. A* **2001**, *105*, 3214. (c) Herges, R. *Chem. Rev.* **2006**, *106*, 4820.
- (9) AICD plots have been utilized in analyses of various porphyrinoids. See: (a) Yoon, M.-C.; Shin, J.-Y.; Lim, J.-M.; Saito, S.; Yoneda, T.; Osuka, A.; Kim, D. *Chem.—Eur. J.* **2011**, *17*, 6707. (b) Higashino, T.; Lim, J. M.; Miura, T.; Saito, S.; Shin, J.-Y.; Kim, D.; Osuka, A. *Angew. Chem., Int. Ed.* **2010**, *49*, 4950. (c) Lee, J. S.; Lim, J. M.; Toganoh, M.; Furuta, H.; Kim, D. *Chem. Commun.* **2010**, 46, 285.
- (10) (a) Chen, Z.; Wannere, C. S.; Corminboeuf, C.; Puchta, R.; Schleyer, P. v. R. *Chem. Rev.* **2005**, *105*, 3842. (b) Schleyer, P. v. R.; Maerker, C.; Dransfeld, A.; Jiao, H.; Hommes, N. J. R. v. E. *J. Am. Chem. Soc.* **1996**, *118*, 6317.
- (11) (a) Song, H.; Cissell, J. A.; Vaid, T. P.; Holten, D. *J. Phys. Chem. B* **2007**, *111*, 2138. (b) Cho, S.; Yoon, Z. S.; Kim, K. S.; Yoon, M.-C.; Cho, D.-G.; Sessler, J. L.; Kim, D. *J. Phys. Chem. Lett.* **2010**, *1*, 895. (c) Lim, J. M.; Yoon, Z. S.; Shin, J.-Y.; Kim, K. S.; Yoon, M.-C.; Kim, D. *Chem. Commun.* **2009**, 261.
- (12) The first oxidation wave of **3** was irreversible and was probably due to the reaction at the α position of the thiophene moiety. The first oxidation potential of **3** was thus determined by differential pulse voltammetry.